RSC Advances

ROYAL SOCIETY OF CHEMISTRY

www.rsc.org/advances

Microwave-induced calatytic Degradation of a Textile dye using Bentonite-Poly(o-toluidine) Nanohybrid

Ufana Riaz* and S.M.Ashraf[1]
Materials Research Laboratory
Department of Chemistry,
Jamia Millia Islamia (A Central University), New Delhi-110025,India
Email: ufana2002@yahoo.co.in
**Corresponding Author*
[1]now retired

Abstract

The present study highlights the potential use of natural clay based organic-inorganic hybrid as an eco-friendly catalyst for the degradation of Malachite Green under microwave irradiation. Bentonite-poly (o-toluidine) nano hybrid was prepared through microwave-assisted solid state in-situ intercalation and polymerization. The intercalation of poly (o-toluidine) was confirmed by X-ray diffraction analysis, while its conducting state was confirmed by UV-visible spectroscopy. Transmission electron microscopic studies revealed that poly (o-toluidine) extracted from the bentonite interlayer space formed nano spheres and tablets of controlled dimensions. The catalytic efficiency of the nanohybrid in degrading Malachite Green under microwave irradiation was investigated in 100 ppm dye solution in presence of 200 mg of the catalyst for different time intervals. The degradation efficiency of the nanohybrid was observed to be as high as 95% in 10 min. Kinetic analysis demonstrated pseudo first order reaction rate with k values equal to 0.17 min^{-1} and 0.19 min^{-1} respectively at 300 nm and 625 nm in presence of nanohybrid catalyst. Liquid chromatography-mass spectroscopy confirmed the degradation of dye into intermediates of molar mass as low as m/z 89 and 58. TOC analysis showed 94% mineralization of the dye in 20 min in presence of nanohybrid catalyst. Thus, this nanohybrid could be used as a benign microwave catalyst for the non-toxic degradation of dyes under microwave irradiation in absence of UV/visible light source.

Introduction

The effluent discharged by various textile industries contains a large number of dyes, increasing the total COD of wastewaters[1]. Some dyes are reported to cause allergy, dermatitis, cancer and mutation in human beings. Moreover, the persistence of colour appearance (at concentration above 1 mg L^{-1}) in treated wastewaters prevents their re-use[2]. Among the lately used methods for mineralization of organic pollutants, photocatalysis and advanced oxidation process (AOP) have received much attention as they are based on the degradation of contaminants. In photocatalysis, the currently used inorganic semiconductors catalysts such as ZnO, and TiO_2 are repoted to be toxic and difficult to remove from the photoreaction environment[3-4].

The extensive use of nano-TiO_2 as photocatalyst has led to growing concerns about its potential environmental impacts. Nano-TiO_2 has been found in the effluent of wastewater treatment plants and exterior facade runoff, both of which ultimately enter natural water systems and result in potential exposure of aquatic organisms to nano-TiO_2[5-7]. Nano-TiO_2 has also been reported to cause toxic effects in algae, fish, mice and human cells in laboratory studies[8-10]. The development of green catalysts is, therefore, a subject of intense investigation. Layered materials based organic-inorganic hybrid using conducting polymers such as polyaniline (PANI), polypyrrole (Ppy) with clays have been extensively investigated for their application in batteries, sensors, organic light emitting diodes (OLEDs) and catalysis[11-15]. Earlier investigations have shown that TiO_2 based conducting polymer/clay nanocomposites enhance degradation of organic dyes under visible radiation[16]. However, the utilization of conducting polymer/clay nanocomposites as a microwave catalyst is an unexplored alternative.

Pillared clays (PILCs) have been used as solid supports for the encapsulation of transition metal complexes to develop heterogeneous catalysts having metal–complex–clay hybrid structure[17]. Studies on heterogeneous photocatalysis of dyes are available in literature[18-19]. Oxidative reagents such as H_2O_2 are always employed in order to promote the degradation process. In this context, *Sanabria et al.*[20] has reported the use of pillared bentonite with solid Al–Fe polyhydroxycation in the catalytic

oxidation of phenol with H_2O_2. *Cheng et al.*[21] also tested the catalytic activity of iron species in layered clays for the photo-degradation of organic dyes under visible irradiation using H_2O_2 as oxidant, while *Feng et al.*[22] reported the use of a bentonite-based Fe nanocomposite film as a heterogeneous photo-Fenton catalyst for the decolourization of orangeII. *Cheng et al.*[23] synthesized a metal–complex–clay material using laponite clay as host and iron(II) 2,2-bipyridine complex as guest, the obtained material has tested as a catalyst in the photodegradation of organic pollutants in the presence of H_2O_2 under visible irradiation. As shown in these works, H_2O_2 is involved with the catalyst (metal–complex–clay) in the decolourization and degradation of pollutants and where UV, visible/solar irradiations accelerate the oxidation reactions. Microwave irradiation has been proved to be an effective, rapid and efficient technique to treat toxic effluents[24]. The microwave in-situ decomposition process developed by *Abramovitch et al.*[25-26] has been use to remediate soils contaminated with toxic metals such as Cd^{2+}, Mn^{2+}, Th^{2+}, Cr^{3+}, and Cr^{6+}. The heating effect of microwave energy accelerates the reaction rate of many chemical reactions, and has also been applied to enhance the reduction of perchlorate in water by elemental Fe[27].

With the aim to replace toxic inorganic semiconductor based photocatalysts with a non-toxic, efficient and an environmentally safe catalyst, the present study reports the synthesis of Bentonite-poly(o-toluidine) nanohybrid via solid state in-situ intercalation and polymerization using microwave irradiation at temperatures, 30 ˚C, 40 ˚C, and 50 ˚C. Poly(o-toluidine) (POT) was chosen as it exhibits improved processability than PANI and is also reported to be non-toxic[28]. Bentonite is nontoxic and is used as an host material and inert support to enhance the structural and physical properties of POT through its confinement in the interlayer galleries[29-30]. The nanohybrids were synthesized under solid-state condition using microwave irradiation as the extensively adopted solution method of intercalation is reported to be inefficient, multistep and cumbersome[29]. The synthesized nanohybrid was investigated by UV-visible, X-ray diffraction (XRD), and transmission electron microscopy (TEM) to explore the effect of temperature and time of microwave irradiation on the electronic, spectroscopic and microstructural characteristics of these materials**.** Malachite Green (MG) was chosen as a model dye for studying the catalytic activity of the nanohybrid because MG is most widely used for coloring purpose, amongst all other dyes of its category. MG has properties that make it difficult to remove from aqueous solutions and it produces detrimental effects in liver, gill, kidney, intestine and gonads[31]. The enhancement of degradation of MG dye by the nanohybrid under microwave radiation was investigated under different conditions of catalyst dosage, catalyst concentration, and dye concentration. Degradation of the MG dye under microwave was also investigated in presence and absence of nanohybrid and was observed to be much slower in absence of the catalyst than in its presence. Degradation was also studied in absence of microwave irradiation. Results revealed that 50 ml of the 100 ppm dye solution was completely degraded by 200 mg of the nanohybrid in 10 min. The degradation of MG dye under microwave was reported to yield non-toxic fragments of low molar mass which was confirmed by LC-MS studies**.**

Experimental Section

Materials

Bentonite (American Colloid Company, USA). The main chemical components of the bentonite were (wt.%): SiO_2–79.2, Al_2O_3–14.92, Fe_2O_3–2.10, CaO–2.28, Na_2O-2.72,K_2O–0.43. The CEC was 0.88 meq/g.O-toluidine (Sigma Aldrich, USA), ferric chloride (Merck, India), N- methyl-2-pyrolidone (NMP) (Merck, India), and methanol (Merck, India) were used without further purification

Microwave-assisted synthesis of Bentonite-POT nanohybrids

Homogeneous mixing of bentonite clay (1g) with varying amounts of o-toluidine (OT) (0.25g, 0.5g, and 1g) followed by the addition of ferric chloride in the mole ratio of 1:1 (monomer: oxidant ratio) was carried out using agate mortar and pestle prior to microwave irradiation. The reaction vessel was placed in the centre of the microwave cavity and was exposed to microwave irradiation for 6 min in Ladd Research Laboratory microwave oven model LBP125-230 (220/230V), power source- 230 V ~50 Hz, energy output-800 W, input power-1,200 W at 30 ˚C, 40 ˚C, and 50 ˚C[29]. The required temperature was set by a ramp controller provided in the microwave oven and was maintained by an inbuilt probe and an on and off mechanism which allowed the microwave generator to be put on and off as soon as the temperature varied. The color of bentonite clay changed from cream to green which indicated the polymerization of o-toluidine within the bentonite galleries. The nanohybrid obtained was repeatedly washed with distilled water and methanol, dried in vacuum oven at 70 ˚C for 90 hours to ensure complete removal of solvent and water. The colour of the nanohybrid obtained was finally green. The nanohybrids so synthesized were designated as Bentonite:POT 1:0.25-30 ˚C, Bentonite:POT 1:0.25-40 ˚C, Bentonite:POT1:0.25-50 ˚C, Bentonite:POT 1:0.5-30 ˚C, Bentonite:POT 1:0.5-40 ˚C, Bentonite:POT 1:0.5-50 ˚C, Bentonite:POT 1:1-30 ˚C, Bentonite:POT 1:1-40 ˚C, Bentonite: POT 1:1-50 ˚C according to the apparent loading of monomer and microwave exposure temperature.

For the degradation studies, three sets of 50 mL solutions of MG dye of concentration 100 mg/L, were prepared by dilution of a stock solution of 500 mg/L and were labeled as MG-100 (total of 18 samples). 200 mg of the chosen nanohybrid was dispersed using orbital shaker (REMI). The solutions were exposed to microwave radiation in Ladd Research Microwave oven model LBP-250, USA. The temperature of the solutions was automatically controlled at 30 ˚C and measured by a temperature probe located at the centre of the beaker. The solutions were stirred by bubbling O_2 into them transported through propylene tubing. The solutions were irradiated in microwave oven in a batch process for 2, 4, 6, 8, and 10 minutes. The concentration was determined against optical absorption from the calibration curve measured at 300 nm and 625 nm.

Results and Discussion

UV-visible spectra were taken on UV-visible spectrophotometer model Shimadzu UV-1800 using NMP as solvent.

X-ray diffraction patterns of the nanohybrids were recorded on Philips PW3710 X-ray diffractometer (Nickel filtered Cu-Kα radiations).

Transmission electron micrographs (TEM) were taken on FEI Morgagni 268 transmission electron micrographs, USA.

The BET surface area of the samples was measured by single point N_2 adsorption measurements at 77 K by means of Micrometrics ASAP 2020.

For detection and identification of degradation products, liquid chromatography-mass spectroscopy (LC-MS) was conducted using a Finnigan LCQ ion trap mass spectrometer equipped with an electro spray ionization interface (ESI) source and operated in negative polarity mode fitted with a Genesis, C-18 column (4.6×250mm) containing 4 μm packed particles (Alltech, Deerfield, Germany). Acetonitrile and 0.03 M ammonium carbonate buffer, pH 7.7, were used as eluents. The diode array detector allowed for concomitant recording of spectra from 200 to 600 nm. The gradient HPLC separation was coupled with LC/MSD trap 6310, ion trap mass spectrometer (Agilent technologies). The experiments were also carried out in triplicate for evaluating the effect of nanohybrid catalyst dosage and initial dye concentration in the degradation of MG.

Mineralization of the dye was determined by measuring the total organic content (TOC) of the degraded dye at 5, 10, 15 and 20 minutes on Shimadzu TOC-5000A total organic carbon analyzer.

Confirmation of loading and conducting state of POT within Bentonite galleries

The XRD diffractograms of Bentonite:POT nanohybrids synthesized at different temperatures are shown in Fig. 1 (a), (b), and (c). The diffractogram of Bentonite:POT 1:0.5, and 1:1 nanohybrids synthesized at 30 °C, Fig. 1(a), revealed a broad hump from 5°-7° close to the d(001) peak of pristine bentonite, $2\theta = 5.7^{\circ}$ which indicated formation of laterally oriented chains in the interlayer space of clay that causes insignificant increase in the gallery height of these nanohybrids[29]. For Bentonite: POT 1:0.25-30 °C, the peak position shifted to higher 2θ values due to some exfoliation of the POT[29]. They all produced some amorphousness in clay structure. The reflection intensity of these nanohybrids is quite revealing.

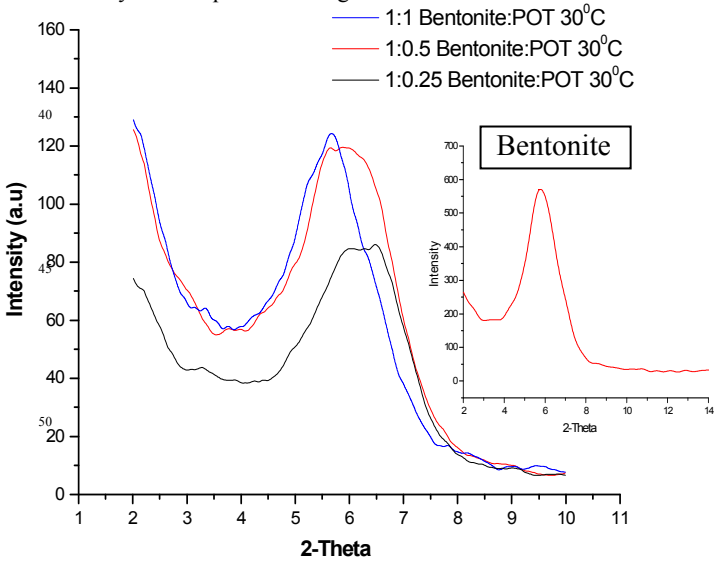

(a)

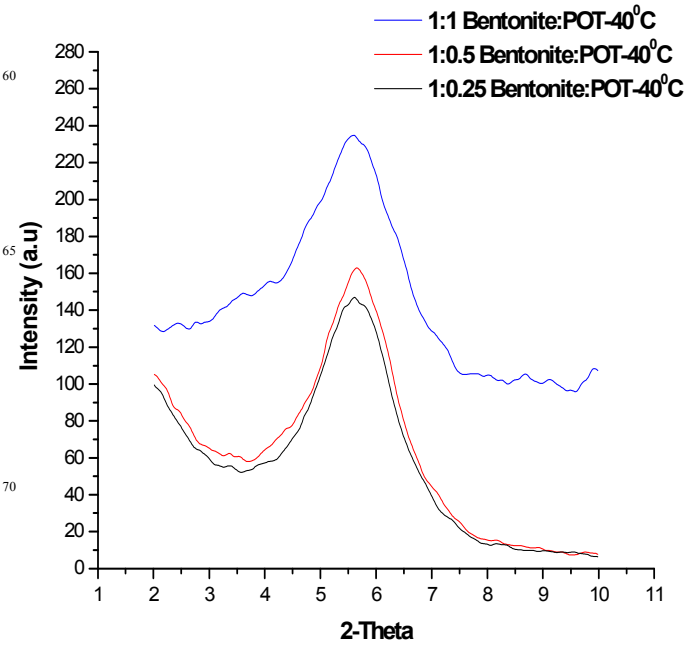

(b)

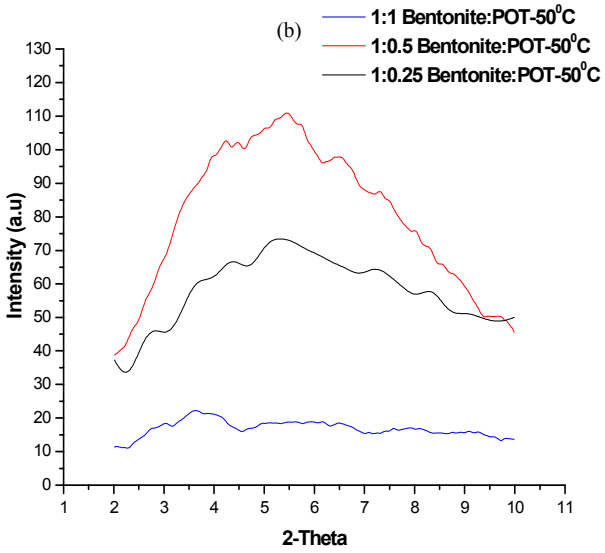

(c)

Fig. 1 XRD diffractograms of Bentonite: POT synthesized at (a) 30 °C (b) 40 °C and (c) 50 °C

The reflection intensity of Bentonite: POT 1:0.25-30 °C was observed to be fairly lower than the other two nanohybrids because of higher out of phase scattering of X-rays by the laterally oriented POT molecules. The diffractograms of Bentonite: POT nanohybrids synthesized at 40 °C, Fig. 1 (b), revealed a well formed peak at $2\theta \approx 5.5^{0}$ for all the three nanocomposites. Small increase in the interlayer space in these cases indicated slightly transverse orientation of the POT chains in the clay galleries. For nanohybrids Bentonite: POT 1:0.25-40°C and Bentonite: POT 1:0.5-40°C, the reflection intensities were the same but lower than Bentonite: POT 1:1.

The higher reflection intensity in case of the later nanohybrid resulted from lower out of phaase of scattering of X-rays by POT chains being slightly transversely oriented. Bentonite:POT 1:0.25 and 1:0.50 nanohybrids synthesized at 50 °C, Fig. 1 (c), revealed broad humps due to higher loading of the POT chains and their transverse orientation that resulted into partial break down of the crystalline structures leading to amorphousness. This confirmed the polymerization and intercalation of POT in the clay galleries. Bentonite:POT 1:1, synthesized at the same temperature, exhibited a highly suppressed diffractogram confirming complete breakdown of the clay structure due to exfoliation of the nanohybrid. From the above observations, it can be concluded that at 30°C and 40°C, all compositions of Bentonite: POT nanohybrid showed polymerization of POT inside the clay galleries with lateral or transverse orientation[29]. Bentonite:POT nanohybrid synthesized at 50°C showed much higher exfoliation and breakdown of crystalline structure of bentonite.

UV−visible spectra of Bentonite:POT nanohybrids are shown in Fig. 2 (a), (b), and (c), while their peak area and oscillator strength values are shown in Table 1. The nanohybrids revealed peaks at 275 nm, 550 nm, and 800 nm. The 550 nm peak is correlated to excitonic transition and 800 nm peak to polaronic transition which are the characteristic peaks of a conducting polymer[16,29]. The presence of polaronic peak confirms the conducting state of POT, inter alia, of nanohybrid. The Bentonite:POT nanohybrids 1:1, 1:0.5, and 1:0.25 showed variation in the absorbance intensity of all the three peaks. Curiously Bentonite: POT 1:0.25 nanohybrid synthesised at 30 °C showed highest absorbance intensity of 2.75 at 800 nm, while Bentonite:POT 1:1-30 °C showed much lower absorbance intensity of 1.5 at this absorption maxima. This property of the former nanohybrid can be exploited in electronic applications.The absorbance intensity of 800 nm for Bentonite:POT 1:0.25 and 1:1 nanohybrids synthesised at 40 °C and 50 °C was found to be respectively 0.9, 0.4; and 0.4, 0.05.With the increase in temperature large decrease in the absorbance intensity of the POT, or, Bentonite: POT nanohybrid was observed. At high temperatures, the crystal structure was severly deformed and the conformation of the POT chains hindered polaron formation in the confined environment of interlayer space under microwave irradiation. Higher value of absorbance intensity of Bentonite:POT 1:0.25 than Bentonite:POT 1:1 at each temperatures resulted from higher transition dipole moment, and correspondingly higher extinction coefficient than the later. Table 1 gives integrated absorption coefficient and oscillator strength of transitions at 800 nm for nanohybrids Bentonite:POT 1:0.25, Bentonite:POT 1:0.5, and Bentonite:POT 1:1 at 30 °C. Integrated absorption coefficient is indicative of net transition dipole moment and oscillator strength already defined in our ealier studies[29]. A large decrease in integrated absorption coefficient of each nanohybrid is noticed with increasing temperature**.** This results from increasing polaron annihilation with increasing temperature because of increased conformational changes in POT chains in the confined environment of bentonite interlayer space[29]. The oscillator strength of Bentonite:POT 1:0.25, 1:0.5, and 1:1 at 30 °C, 40 °C, and 50 °C respectively showed following values: 0.026, 0.023, 0.016; 0.010, 0.008, 0.005; and 0.004, 0.005, 0.002. Since integrated absorption coefficient decreased with temperature, the oscillator strength was also found to show the same behaviour. It can be interestingly noticed that at each temperature, oscillator strength decreased as POT loading increased in the nanohybrid. Thus oscillator strength of Bentonite:POT 1:0.25 was higher than that for Bentonite: POT 1:1. At lower loading in Bentonite:POT 1:0.25, the POT chains are distributed discretely and laterally in the clay galleries. Hence, the net transition dipole moment will vectorially add up, and the oscillator strength will be higher. At higher loading, Bentonite:POT 1:1, the POT molecules are oriented transversely and may have different conformations. Some components of the transition dipole moments will vectorially cancel each other, resulting in the lower value of net transitional dipole moment. This will cause the oscillator strength to be low in this case. These observations have implications in nanohybrid's electronic applictions.

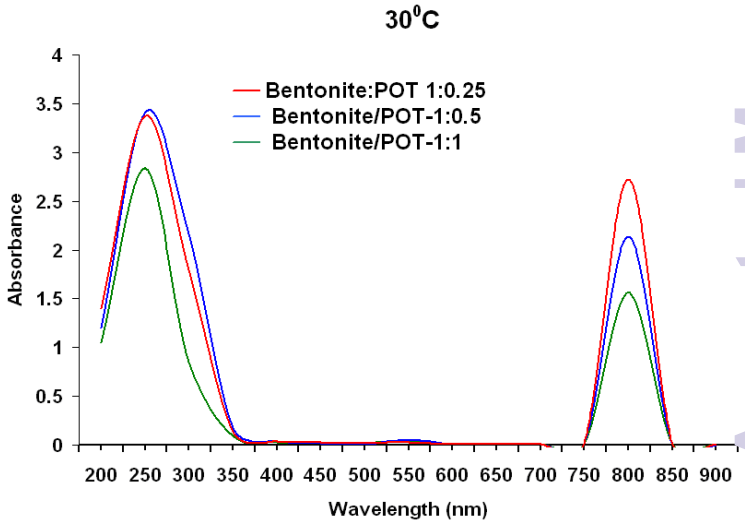

(a)

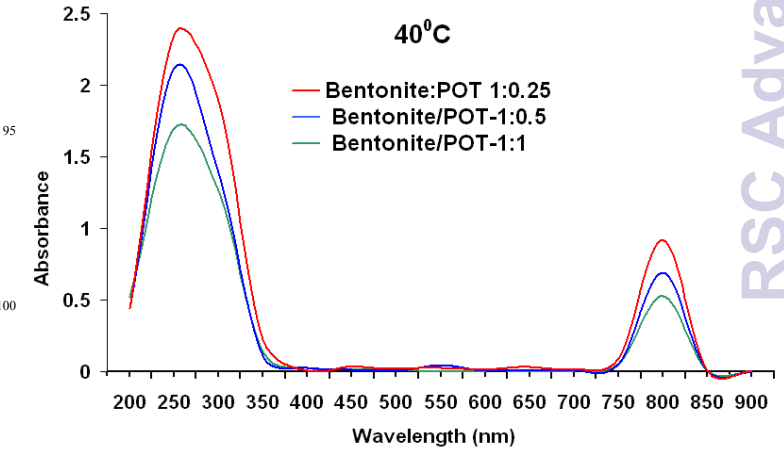

(b)

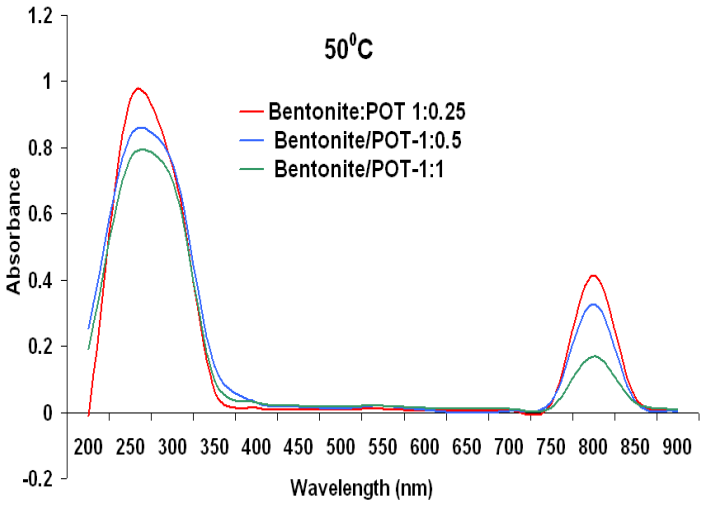

(c)

Fig.2 UV-visible spectra of Bentonite:POT nanocomposites synthesized at different temperatures

Table .1 Oscillator strength and peak area values of Bentonite: POT nanohybrids synthesized at different temperatures

Sample	λ_{max} (nm)	Peak area $\int ad\bar{\nu}$	Oscillator Strength
Bentonite:POT -30 °C			
Bentonite:POT 1:0.25	800	92.76	0.026
Bentonite:POT 1:0.5	800	88.53	0.023
Bentonite:POT 1:1	800	67.47	0.016
Bentonite:POT -40 °C			
Bentonite:POT 1:0.25	800	37.06	0.010
Bentonite:POT 1:0.5	800	29.97	0.008
Bentonite:POT 1:1	800	21.07	0.005
Bentonite:POT -50 °C			
Bentonite:POT 1:0.25	800	26.12	0.004
Bentonite:POT 1:0.5	800	22.15	0.003
Bentonite:POT 1:1	800	10.20	0.002

Morphology of the synthesized nanohybrids

The TEM micrographs of Bentonite:POT nanohybrids synthesized at 30 and 40 °C are depicted in Fig. 3 (a), (b), (c), and (d). The nanohybrid Bentonite:POT 1:0.25-30 °C, Fig.3 (a), shows formation of small spherical and also flexible fiber like particles in the clay indicating that POT molecules self-assemble themselves in different geometrical forms**.** These nanoparticles vary in size from 65-100 nm. The clay appears as a sheet in this micrograph. The later reveals separation of layers in clay particles. Bentonite:POT 1:0.5-40 °C, Fig. 3 (b), also shows sheet structure of clay and aggregates of POT fibers. Since XRD, Fig. 1 (b), does not explicitly reveal exfoliation, it can be inferred that dispersion of Bentonite:POT nanohybrid in water brings about separation of layers of clay particles as has been observed by other authors[32-33]. Upon extraction of POT from Bentonite using the procedure mentioned in our earlier studies, predominantly spherical and also tablet like particles both in case of Bentonite:POT 1:0.25-30 °C and Bentonite:POT 1:0.5-40 °C, of around 75 nm were observed. All the particles appear to be nearly of the same size and morphology which confirms the controlled growth of POT outside bentonite galleries. It appears that spheres and tablets are formed by the self-assembly of fibers of POT particles. Self-assembly of POT inside the bentonite galleries takes place through the coiling of POT chains. The hydrophobic interactions between the OT units of POT chains impart stability to the small spherical and fiber like structure of POT particles, Figs. 3 (a), (b), (c), and (d). Based on the spectroscopic and morphological studies, Bentonite:POT-30 °C nanocomposites were chosen for surface studies**.**

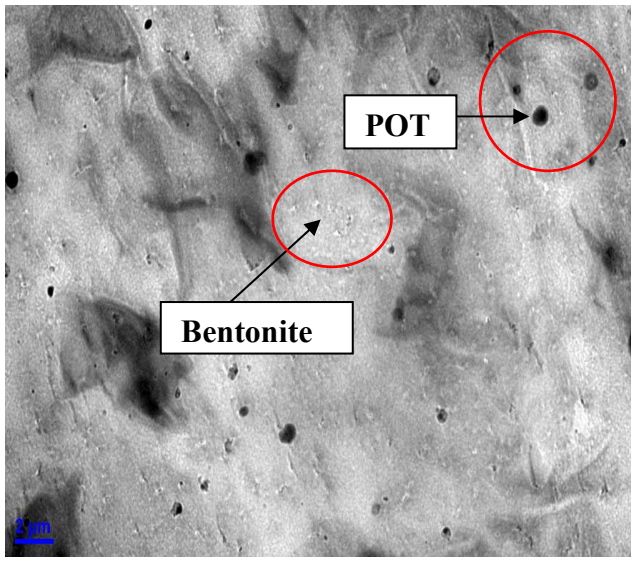

(a)

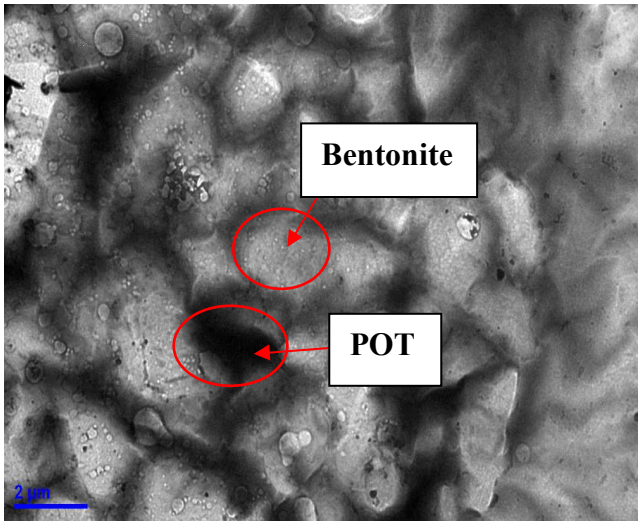

(b)

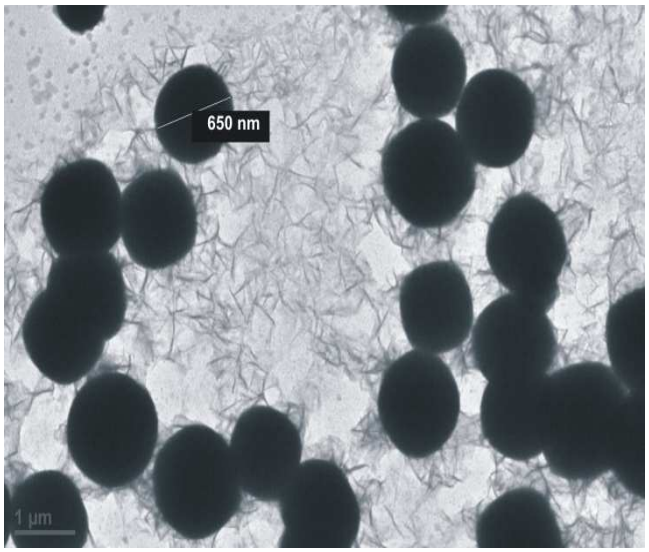

(c)

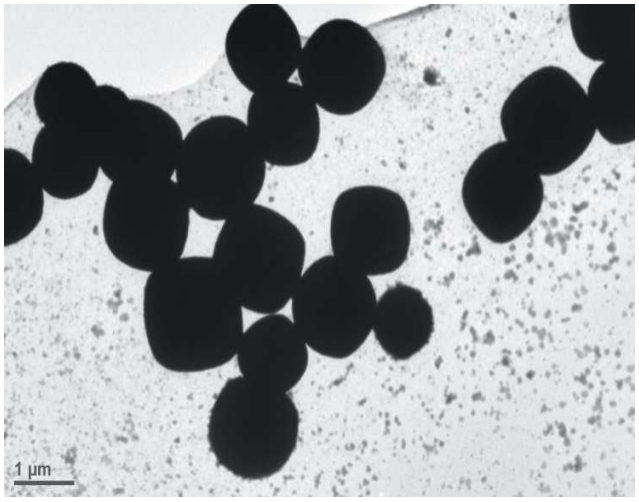

(d)

Fig.3 TEM micrographs of (a) Bentonite: POT 1:0.25-30 °C, (b) Bentonite: POT 1:0.5-40 °C, (c) Bentonite: POT 1:0.5-30 °C (POT extracted from Bentonite), (d) Bentonite: POT 1:0.5-40 °C (POT extracted from Bentonite)

Surface studies and catalytic properties of Bentonite:POT nanohybrids

The surface area data showed that the nanohybrids possesed higher surface area than pure bentonite, Table 2. The nanohybrid Bentonite:POT 1:0.25-30°C showed surface area 120 m^2 g^{-1} which was noticed to be higher than bentonite 88 m^2 g^{-1}. This increase resulted from some separation of clay platelets upon intercalation of POT. The nanohybrid Bentonite:POT 1:0.5-30 °C indicated a surface area of 140 m^2 g^{-1} because of higher separation of clay platelets due to higher loading of POT[32-33]. The decrease in the surface area of the nanohybrid Bentonite:POT 1:1-30 °C is caused by the tactoid formation of the clay platelets because of higher loading. Based on the surface properties, Bentonite:POT 1:0.5-30 °C was chosen for catalytic studies.

Table 2 Surface area of the nanohybrids

Samples	Surface area (m^2 g^{-1})	Particle size (nm)
Bentonite	88	250
Bentonite:POT 1:0.25-30°C	120	170
Bentonite:POT 1:0.5-30°C	140	100
Bentonite:POT 1:1-30°C	103	210

Catalytic performance was measured through degradation of malachite green (MG) under microwave irradiation for 2, 4, 6, 8, and 10 min by monitoring UV-visible absorbance intensity of the degraded dye samples at the above times. The dye solutions were equilibrated with the catalyst for 72 hours prior to the microwave irradiation and the degradation in absence of any microwave irradiation was monitored at different intervals of time.A small decrease (4%) in the intensity of the 625 nm peak of MG was observed due to the absorption of dye on the catalyst surface. The degradation of MG was followed by measuring the absorbance intensity of the dye solutions at different intervals at its 300 and 625 nm peaks[31,34]. The concentration of the dye at any interval was determined by matching the absorbance intensity on a calibration curve. The ratios of C, the concentration of dye at different times of microwave exposure to the initial concentration Co of the dye, C/Co, were plotted against the time of microwave exposure, t, to compare the efficiency of the degradation under different conditions. Equilibriation prior to the beginning of each experiment discounted any error due to adsorption.

The C/C_0 plot of 100 ppm dye solution for pure bentonite, pure POT and the nanohybrid is shown in Fig. 4 (a), and (b). The blank dye solution, Fig. 4 (a), revealed a degradation of 10% of MG after 10 min of microwave exposure at 300 nm while at 625 nm it showed the same as 11%. Pure POT caused 13% degradation of MG at the 300 nm and 14% degradation at 625 nm, Fig. 4 (a). The C/C_0 plot of pure bentonite, Fig. 4 (b), revealed a degradation of 25% of MG after 10 min of exposure at 300 nm whereas for the 625 nm peak, the same was found to be 35%. In presence of the nanohybrid catalyst, at 300 nm peak, the degradation efficiency increased to 75%, while at the 625 nm peak it rose to 95%.

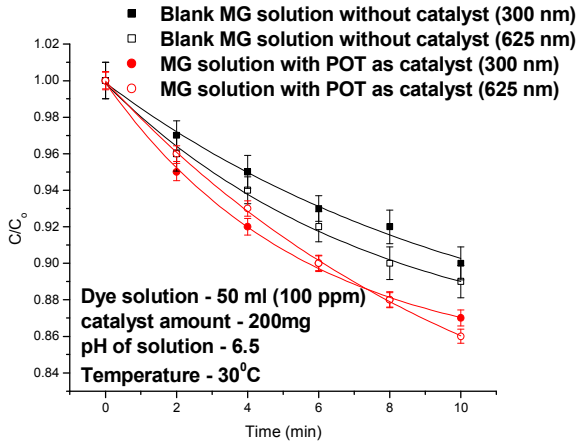

(a)

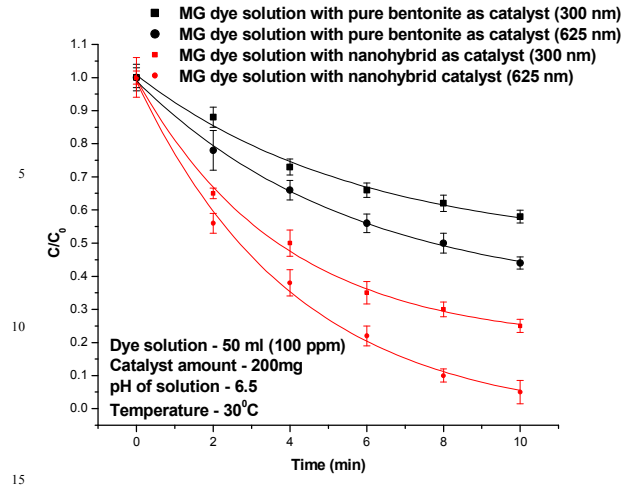

(b)

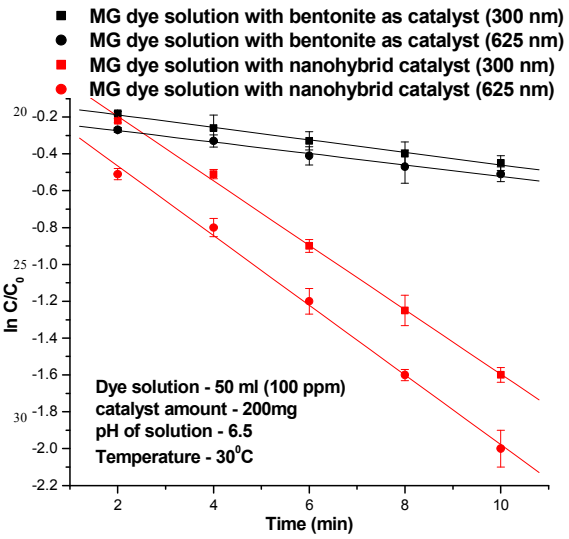

(c)

Fig. 4 plot of C/Co vs. time for (a) MG dye solution in absence of any catalyst and in presence of pure POT as catalyst, (b) in presence of pure bentonite and bentonite: POT nanohybrid as catalyst (c) ln C/Co vs. time for bentonite and bentonite:POT nanohybrid

Since we found that the degradation of the MG dye in presence of catalyst was substantial than in absence of catalyst while in presence of pure bentonite it was appreciable, the degradation the dye in the later two has been kinetically analyzed.

The plot of ln (C/C_0) vs. time for Bentonite:POT 1:0.25-30 °C, Fig. 4 (c), revealed a pseudo first order reaction. The rate constant (k) values at 300 nm and 625 nm were found to be 0.02 min^{-1} and 0.024 min^{-1} respectively in presence of pure bentonite, and 0.17 min^{-1} and 0.19 min^{-1} respectively in presence of the nanohybrid catalyst. These values showed higher rate of degradation of the dye in presence of nanohybrid catalyst.The mechanism for the degradation of MG in presence of nanohybrid can be explained as follows. One photon of microwave radiation has the energy ≈ 10^{-5} eV which is several orders of magnitude smaller than the energy required for breaking a C-C or a C-H covalent bond, respective dissociation energies of the two bonds being 3.6 eV and 4.3 eV; the excitation energy of an electron from HOMO to LUMO in a conducting polymer is ≈ 3.0 eV. Hence microwave alone cannot excite electron from a conducting polymer and create charge carriers. Similarly, microwave radiations alone cannot bring about fission of C-C and C-H bonds through which chemical reactions occur. In a polar solvent, microwave radiation produces high temperature known as "thermal effect" through dielectric heating which allows chemical reactions to occur at very fast speed[35]. But water in this case splits into H_2 and O_2 molecules due to high temperature. Catalytic degradation of the dye into intermediates of low molar masses will, therefore, occur through involvement of $OH^{\bullet}$ and $H^{\bullet}$ free radicals. Since charge separation can not occur under microwave irradiation in POT, this semiconductor will not be able to produce electrons and holes which in turn will not be able to produce $OH^{\bullet}$ and $H^{\bullet}$ free radicals.As dye degradation has been observed experimentally above and in LC-MS studies reported in a later section, it takes place definitely through the involvement of $OH^{\bullet}$ and $H^{\bullet}$ free radicals[35-36]. The microwave oven used in this study is run at fairly low temperature, 30 °C, unlike conventional microwave ovens. Hence, $OH^{\bullet}$ and $H^{\bullet}$ free radicals are presumed to be formed by splitting of H_2O molecules through nonthermal effect of microwave radiation. *Horikoshi et al.* [36-37] and *Zhang et al.*[38] have observed non-thermal effect of microwave radiation in enhancing the rate of dye degradation in several studies. The nanohybrid Bentonite:POT 1:0.5-30 °C showed highest optical and electronic transition characteristics among the other nanohybrids. This nanohybrid is expected to cause perturbation in the surface electronic states which augments the charged state of the nanohybrid surface. This enhances active adsorption sites on the Bentonite:POT nanohybrid surface.

The water molecules are copiously adsorbed on negatively charged site of the nanohybrid surface, Scheme.1. Under microwave irradiation, the water molecules are subjected to orientation polarization but electrostatic attraction between the two oppositely charged polar groups (Scheme 1) does not permit the water molecules to flip. This will produce enormous strain in OH bonds of water molecules. Since the two hydrogens will not be pulled by equal force by the negatively charged oxygen of the nanohybrid, charge density not being equal at all the negative sites because of perturbation; water molecules will split into $H^{\bullet}$ and $OH^{\bullet}$ free radicals. Other undefined non thermal effect may also have contributed to the splitting of water molecules into $OH^{\bullet}$

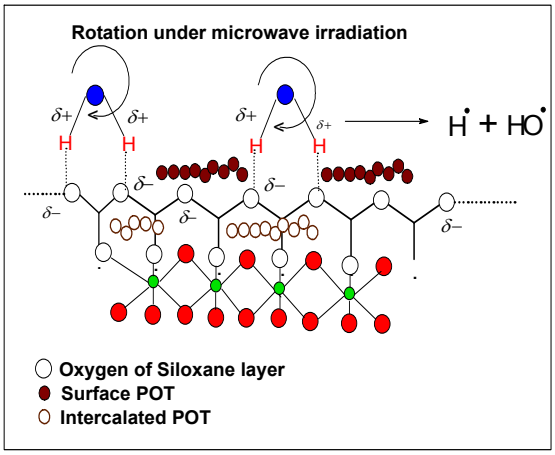

Scheme 1.Oritentation polarization of water molecules in presence of microwave and nanohybrid

and H• free radicals. The OH• and H• free radicals attack dye molecules around the the nanohybrid surface and in the bulk and degrade them. The presence of OH• free radicals and its participation in the degradation of the dye molecules was confirmed by isopropyl alcohol, a scavenger of OH•. When isopropyl alcohol (5 mmol/ L) was added in the 100 ml of MG solution and exposed to microwave radiations, in presence of 200 mg catalyst, the degradation of dye was completely stopped as no decrease in the intensity of the characteristics peaks of MG was noticed. Using isopropanol, in absence of microwave irradiation, but in presence of bentonite, the decrease in absorbance intensity of the dye solution was the same; as it was in absence of isopropanol.Decrease in absorbance intensity could not be stopped by isopropanol. This showed that the degradation of dye did not occur in absence of microwave irradiation as no free radicals were formed.

The degradation continues till mineralization of the dye. The dye was also found to degrade in the absence of nanohybrid catalyst, Fig. 4 (a). In this case the water molecules adsorbed on the glasss surface split into H• and OH• free radicals by the samee mechanism as described above. We have also investigated thee effect of initial MG dye concentration and the nanohybrid dosage on the degradation efficiency of the dye. The effect of initial dye concentration, which was varied from 50-400 ppm, on the degradation of MG is illustrated in Fig. 5. It was observed that for 50 ppm dye solution, degradation was higher for 100 ppm dye solution than for 200 ppm solution in presence of catalyst. It then decrease slowly. In the absence of catalyst, degradation efficiency was 35% with 100 ppm, while with 200 ppm it was 15%. The effect of the nanohybrid catalyst dosage in 50 ml of 100 ppm MG dye is shown in Fig. 6. As the catalyst dosage was increased, an increase in the efficiency was observed upto 200 mg. At and beyond this amount, the degradation efficiency was 95%.

Thus, the final degradation efficiency did not change, showing that the excess amount of the catalyst could not improve the degradation efficiency in the microwave-assisted degradation of MG dye**.** After the first run, the catalyst was separated by centrifugation, washed thoroughly with deionised distilled water repeatedly for three times. The presence of any dye in the supernatant solution was checked spectrophotometrically. This was followed by washing with methanol and drying it in vacuum oven at 60 ^{0}C for one hour.

The catalyst was then reused for further runs**.** The results show that upto eight cycles, the activity of catalyst did not exhibit any significant loss. It indicates that the Bentonite: POT nanohybrids have high stability and reusability. Moreover the catalyst could be easily recovered by centrifugation and decantation. Thus, the easy recovery and reusability of Bentonite: POT proves its practical application as a microwave-catalyst.

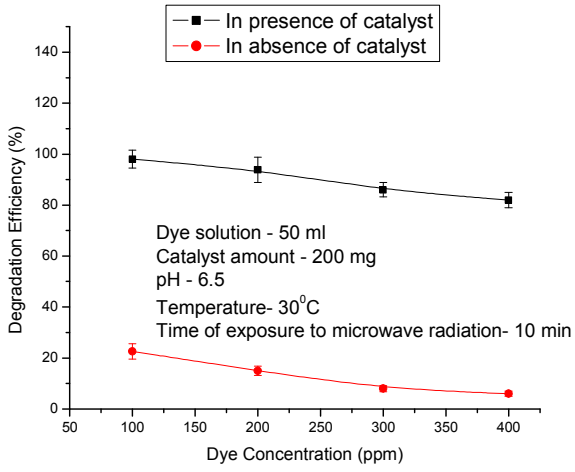

Fig. 5 Effect of concentration of MG dye on its degradation in presence

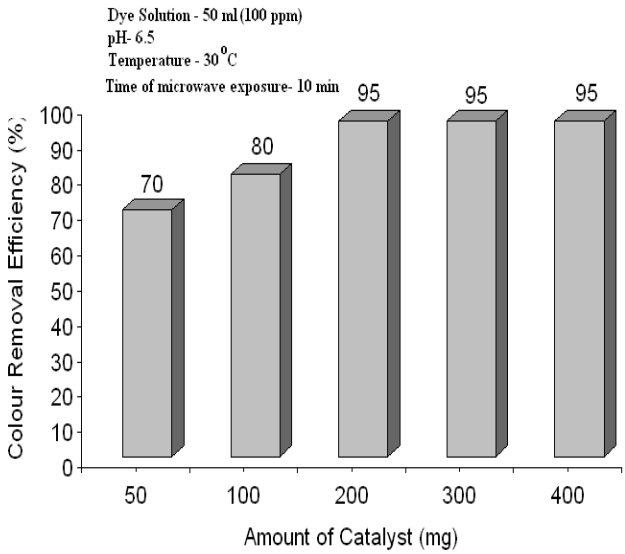

Fig. 6 Effect of the amount of nanohybrid as catalyst on the degradation efficiency

Degradation product analysis

Catalytic degradation of MG dye was further confirmed through analyzing the partially degraded samples of the dye by LC-MS method. In the first step degraded sample was subjected to HPLC analysis. HPLC results showed peaks at differen retention times. MS analysis of fractionated dye samples at different retention times were carried out and the resuts are shown in Table 3. It was obseved that dye degraded successively into intermediates of decreasing m/z values. The intermediates with lowering m/z values, 245, 233, 113, 103, 89, 58 with corresponding molecular structures are shown in Scheme 2 which represnts the degradation pathway.

Table 3 Intermediates found at different retention times

Retention time	Intermediates with % abundance
Bentonite:POT (1:0.5-30°C)	
MG-100	
5 min	58 (100%), 113 (50%)
12 min	113(100%), 245 (78%), 103 (48%)
MG-100	
10 min	89 (100%), 329 (84%),
16 min	233 (100%), 245 (86%), 103 (83%), 89 (63%), 58 (35%)

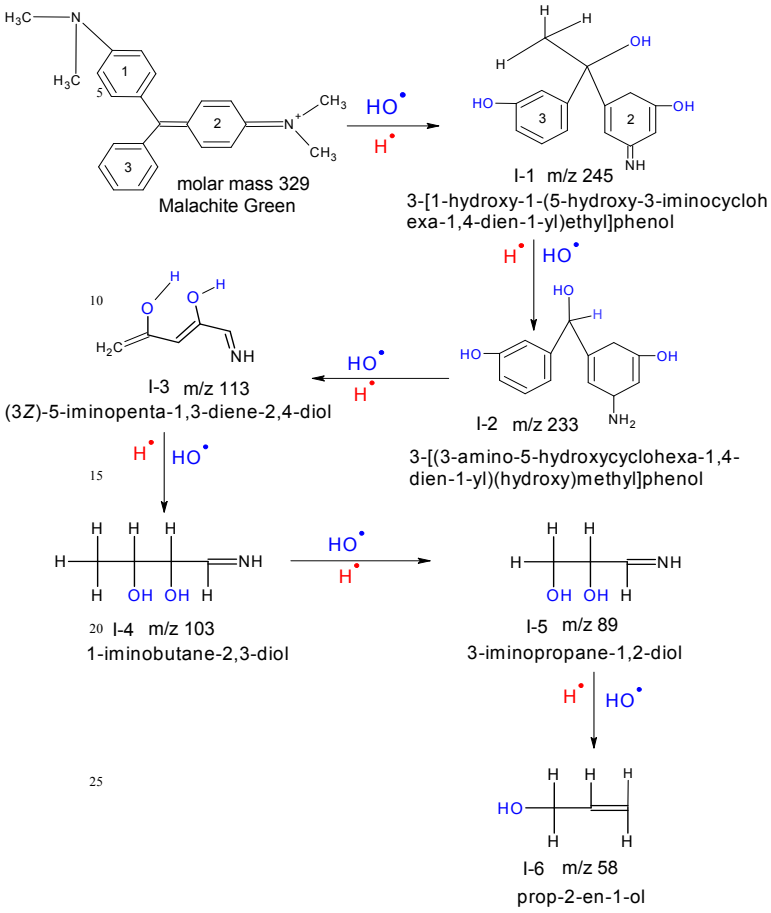

Scheme 2 Degradation pathway of MG in presence of nanohybrid

They are successively labelled as I-1, I-2, I-3, I-4,and I-5, and I-6 and the parent dye as M-1. Above m/z 245, no prominent intermediate was found.We have therefore taken I-1, m/z 245, as the intermediate from parent dye M-1 which generated the intermediates from I-2 to I-6. The intermediates revealed that degradation proceeded via elimination of methyl groups, amino group, asymmetric cleavage of benzene rings, all, through attack of $OH^{\bullet}$ and $H^{\bullet}$ free free radicals. Unpreferrential attack of $OH^{\bullet}$ and $H^{\bullet}$ free free radicals on carbons of benzene rings resulted in their cleavage and oxidation. I-1, (m/z 245), [3-[1-hydroxy-1-(5-hydroxy-3-iminocyclohexa-1,4-dien-1-yl)ethyl]phenol] was obtained from parent dye M-1 by elimination of dimethyl amino group, cleavage and oxidation of benzene ring 1 by attack of $OH^{\bullet}$ and $H^{\bullet}$ free radicals to be reduced into a bridge group of $(CH_3)C$ (2C) (OH), and oxidation of dimethyl ammonium group of benzene ring 2, ultimately into NH group. I-1, m/z 245, degraded into I-2, (m/z 233) [3-{(3-amino-5-hydroxycyclohexa-1,4-dien-1-yl)(hydroxy)methyl}phenol] by elimination of CH_3 group through attack of $H^{\bullet}$ free radical on the bridge group $(CH_3)C$ (2C) (OH) of I-1. One OH group is also added on benzene ring 3 through $OH^{\bullet}$ free radical attack. I-3, (m/z 113), [(3Z)-5-iminopenta-1,3-diene-2,4-diol] was obtained by degradation of I-2. In this case I-2 undergoes transfrmaion by fission at bridge C and C-2 of benzene ring 3 by attack of $H^{\bullet}$ and $OH^{\bullet}$ free radicals and further fission at C-6 and C-5 of benzne ring 2 by reactions of $H^{\bullet}$ and $OH^{\bullet}$ free radicals.These reactions ultimately produce I-3, a linear chain unsaturated aliphatic dihydroxy amine of m/z value of 113. Elimination of the end carbon of I-3 through attack of $H^{\bullet}$ free radicals formed intermediate I-4, (m/z 103) [1-iminobutane-2,3-diol]. Elimination of again end carbon of I-4 through attack of $H^{\bullet}$ free radicals produced I-5, (m/z 89) [3-iminopropane-1,2-diol]. The later degraded into intermediate I-6, (m/z 58) [prop-2-en-1-ol] by elimination of terminal NH group expectedly as NH_2OH through attack of $OH^{\bullet}$ and $H^{\bullet}$ free radicals. The last intermeditae degraded into lower alkane and alcohol molecules, at the pattern of previous degradation steps, leading to mineralisation. Table 3 shows that catalyst degraded the dye into much smaller fragments as compared with degradation products in its absence in the same time. Since the degradaiton products are mainly linear chain unstaurated alkanes and alcohols which are found to be toxic, TOC analysis at different times of degradation has been done to find out the extent of mineralization and remaining organic content, Fig.7. It was found that after 20 min of degradation, the organic content left in the dye solution was only 6 %. This indicates nanohybrid catalyst almost mineralizes the dye and toxic products left are negligible. Hence this nanohybrid can be adopted for the safe degradation of toxic dyes.

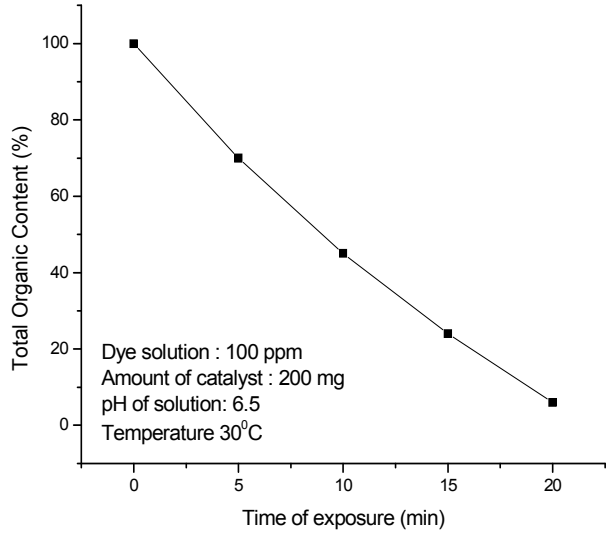

Fig.7 TOC analysis at different times of degradation

Conclusion

Organic-inorganic nanohybrid catalyst, Bentonite-poly (o-toluidine), was developed to replace extensively used nanosized but potentially toxic TiO_2, ZnO and other inorganic semiconductor photocatalysts. This nanohybrid catalyst stands as a potential candidate for environmental remediation under microwave irradiation even in absence of UV/visible light. Poly(o-toluidine) functionalised bentonite showed remarkable catalytic and optical properties. The nanohybrid Bentonite:POT 1:0.5-30 °C was found highly effective catalyst for the degradation of dyes under microwave irradiation alone. Bentonite:POT 1:0.5-30 °C nanohybrid demonstrated high catalytic activity. It completely degraded the 100 ppm Malachite Green dye solution in 10 min. Degradation followed pseudo first order rate kinetics with rate constant, k, values equal to 0.17 min^{-1} and 0.19 min^{-1} respectively at 300 nm and 625 nm in presence of nanohybrid catalyst. In presence of only pure bentonite, the k values were found to be 0.02 min^{-1} and 0.024 min^{-1} at 300 nm and 625 nm respectively. LC-MS analysis showed degradation of Malachite Green into intermediates of so low a molar mass as m/z 89 and 58 which minerallised ito CO_2 and water upto 94%. The degradation of the dye was confirmed to occur through hydroxyl and hydrogen free radicals generated under microwave irradiation by splitting of H_2O molecules. In addition to its optical and electronic properties, this low cost environmentally benign nanohybrid may find suitable application as a green microwave catalyst.

Acknowledgement

The corresponding author Dr.Ufana Riaz also wishes to acknowledge the University Grants Commission (UGC) F.NO 41-199/2012(SR) for granting the UGC Major Research Project.The corresponding author Dr Ufana Riaz also wishes toacknowledge the Department of Science and technology (DST)-science and engineering research board DST-SERB, Indiavide sanction no. SB/S-1/PC-070-2013 for granting major research project.

References

1. V.K.Gupta, A.Mittal, V.Gajbe, *J.Colloid Interf.Sci*. 2005,**284**, 89-98.
2. V.K. Gupta, I.A.Suhas, D.Mohan, *J. Colloid Interf. Sci*. 2003,**265**,257-264.
3. O.Bondarenko, K.Juganson, A.Ivask, K.Kasemets, M.Mortimr, A.Kahru, *Arch.Toxic*., 2013,**87(7)**,1181-1200.
4. J. Feng, X.Hu, P.L. Yue, *Environ. Sci.Technol*. 2004, **38**,269-275.
5. M.A. Kiser, P.Westerhoff, T.Benn, Y.Wang, J.P.Rivera, A. Hristovski, *Environ. Sci. Technol*. 2009, **43**, 6757-6763.
6. Y.Wang, P.Westerhoff, K.D.Hristovski, *J.Hazard.Mater.* 2012, **201-202**,16-22.
7. R. Kaegi, A.Voegelin, B.Sinnet,S. Zuleeg,H.Hagendorfer, M.Burkhardt , and H.Siegrist, *Environ. Sci. Technol.*, 2011, **45 (9)**, 3902-3908.
8. K.H.Rinke,M.Simon,*Env.Sci..Poll.Res*., 2006,**13(4)**,225-232.
9. N. Strigul,L. Vaccari, C.Galdun, M.Wazne, X.Liu, C. Christod oulatos, K.Jasinkiewicz, *Desalination,* 2009,**248(1-3)**,771-782.
10. T.C.Long, N.Saleh, R.D.Tilton, G.V.Lowryand B.Veronesi, .*E*nviron. Sci. Technol., 2006, **40(14),**4346-4352.
11. S.Wang,Y.Kang, L.Wang, H.Zhang, Y.Wang, Y.Wang, *Sens.Actuat.B Chem*., 2013,**182**, 467-481.
12. F-R.Fan, L.Lin, G.Zhu, W.Wu, R.Zhang, and Z.L. Wang, *Nano Lett*., 2012,**12(6)**,3109-3114.
13. T.Griesser, S.V. Radl, T.Koepplmayr, A.Wolfberger, M. Edler, A.Pavitschitz, M.Kratzer, C.Teichert, T.Rath, G.Trimmel, G.Schwabegger, C.Simbrunner, H.Sitter and W.Kern, *J.Mater.Chem*.2012,**22**, 2922-2928.
14. N.Menegazzo , D. Boyne , H. Bui , T.P. Jr.Beebe, K.S. Booksh, *Anal. Chem*.2012, **84 (13)**,5770-5777..
15. R.T. Tsuchiya, S. Hirata, and T.D.Iordanov, *J.Phys.Chem. A*, 2012,**116 (49)**,12153-12162.
16. S.Ameen, M.S.Akhtar, Y.S.Kim,O-B.Yang,H-S.Shin, *Coll.Polym.Sci.* 2011,**289**,415-421.
17. V.Ramaswamy, M.S.Krishnan, A.V. Ramaswamy,*J.Mol. Catal. A*, 2002,**181**,81–89.
18. X.Xu, L.Feng, H.Zhuangqun, *Rev.Adv.Sci.Engg*., 2014, 3(2), *158*-171.
19. M.A.Vicente, C.Belver, R.Trujillano, V.Rives, A.C. Alvarez, J.-F.Lambert, S.A.Korili, L.M.Gandı˘ıa, A.Gil, *Appl. Catal. A: Gen.* 2004,**267**,47–58
20. N.Sanabria, A.Alvarez, R.Molina, S. Moreno,*Catal. Today*, 2008,**133–135**,530–533.
21. M.Cheng, W. Song, W. Ma, C.Cheng, J.Zhao, J.Lin, H.Zhu, *Appl. Catal. B*, 2008,**77**,355–363.
22. J.Feng, X.Hu,P.L. Yue, *Water Res.* 2005,**39**,89–96.
23. M.Cheng,W.Ma,C.Chen, J.Yao,J.Zhao, *Appl. Catal. B: Environ.* 2006,**65**,217–22.
24. T.J.Appleton, R.I. Colder,S.W.Kingman,I.S.Lowndes, A.G. Read, *Appl.Energy*,2005,**81(1),**85-113.
25. R.A.Abramovitch,L.C.Qing, E.Hicks,J.Sinard,*Chemosphere*, 2003,**53(9)**, 1077-1085.
26. R.A.Abramovitch, H.B.Zhou,M.Davis,L.Peters,*Chemosphere*, 1998,**37(8)**, 1427-1436.
27. S-Y. Oh,P.C.Chiu,B.J.Kim,D.K. Cha,*J.Hazard.Mater.*2006, **129(1-3)**,304-307.
28. G.M.Sudhana, G.Thenmozhi, D.Jayakumar and R.J. Santhi,*J.Chem.Pharmaceut.Res*., 2012, **4(1)**, 491-500.
29. U.Riaz,S.M. Ashraf, *J.Phy.Chem C* 2012, **16(22)**, 12366-12374.
30. P.Baláž, M.Achimovičová, M.Baláž, P.Billik,Z.C.Zheleva, J.M.Criado,F.Delogu,E.Dutková, E.Gaffet,F.J.Gotor, R. Kumar, I.Mitov, T.Rojac, M.Senna,A.Streletskii, and K.W. Ciurowa, *Chem. Soc. Rev*., 2013,**42**, 7571-7637.
31. V.K. Gupta, A. Mittal, L.Krishnan, V.Gajbe, *Sep.Purif. Technol.* 2004, **40**, 87-96.
32. F.L.Arbeloa, J.M.H.Martínez, T.L.Arbeloa, and I.L. Arbeloa, *Langmuir*, 1998, **14 (16)**, 4566-4573.
33. F.L.Arbeloa,M.J.T.Estevez, T.L.Arbeloa,I.L.Arbeloa, *Langmuir*, 1995, **11(8),**3211-3217.
34. N.J.B. Pe´rez, M.F.S. Herrera, *Ultrason.Sonochem.* 2008,**15**,612-617.
35. C.O.Kappe, D.Dollinger, *Chem.Rev.* 2001,**107**,2563-2591.
36. S.Horikoshi, A.Saitou, H.Hidaka,N.Serpone,*Environ.Sci. Technol.* 2003,**37(24)**,5813-5822.
37. S.Horikoshi, H.Hidaka, N.Serpone, *J.Photochem.PhotoBiol.A*, 2004,**161(2-3)**,221-225.
38. X.Zhang, D.D.Sun, G.Li, Y.Wang, J.*Photochem.PhotoBiol.A* 2008, **199(2-3)**,311-315.